Journal of NeuroVirology, 9: 530–538, 2003

ISSN: 1355-0284 print / 1538-2443 online
DOI: 10.1080/13550280390241160

Taylor & Francis
Taylor & Francis Group

Provirus expansion and deregulation of apoptosis-related genes in the spinal cord of a rat model for human T-lymphocyte virus type I–associated myeloneuropathy

Utano Tomaru, Hitoshi Ikeda, Xiuyun Jiang, Osamu Ohya, and Takashi Yoshiki

Department of Pathology/Pathophysiology, Division of Pathophysiological Science, Hokkaido University Graduate School of Medicine, Sapporo, Japan

Apoptosis of the spinal oligodendrocytes is the main factor linked to the pathogenesis of human T-lymphocyte virus type I (HTLV-I)–induced myeloneuropathy in rats (HAM rat). To clarify apoptosis-related mechanisms, expression of apoptosis-related genes in the spinal cord of these rats was chronologically examined by means of a semiquantitative reverse transcriptase–polymerase chain reaction. Provirus expansion and increment of HTLV-I *pX* mRNA were evident at 7 months after the induced infection. Tumor necrosis factor-α increased gradually soon after *pX* expression. The expression of a major apoptosis-resistant gene, *bcl-2*, was markedly suppressed at a period of the provirus expansion and *bax* was also down-regulated. *p53* was consistently expressed at high levels. These findings were never observed in spinal cords of HAM-resistant strains with HTLV-I infection even throughout their entire life. Collective evidence suggests that the local provirus expansion and deregulation of apoptosis-related genes, especially down-regulation of *bcl-2*, may lead to apoptosis of oligodendrocytes, thus being a major pathogenetic pathway in the HTLV-I–induced myeloneuropathy. *Journal of NeuroVirology* (2003) **9,** 530–538.

Keywords: apoptosis-related genes; bcl-2; HTLV-I–associated myeloneuropathy; rat model; virus expansion

Introduction

Human T-lymphocyte virus type I (HTLV-I) causes adult T-cell leukemia (ATL) (Poiesz *et al*, 1980; Yoshida *et al*, 1982) and HTLV-I–associated myelopathy/tropical spastic paraparesis (HAM/TSP) (Gessain *et al*, 1985; Osame *et al*, 1986), and is also suggested to be causally related with a number of disorders (Hollsberg and Hafler, 1993), including HTLV-I–associated uveitis (Mochizuki *et al*, 1992), HTLV-I–associated arthropathy (Nishioka *et al*, 1989), Sjögren's syndrome (Vernant *et al*, 1988), and probably T-cell alveolitis (Sugimoto *et al*, 1987), polymyositis (Morgan *et al*, 1989), and infective dermatitis (LaGrenade *et al*, 1990). To investigate the pathogenesis in these diverse disorders, we developed a rat model. Chronic progressive myeloneuropathy, designated as HAM rat disease, was induced in Wistar-King-Aptekman-Hokudai (WKAH) strain rats by HTLV-I infection, after a long incubation period (Ishiguro *et al*, 1992). Although six other rat strains could become carriers of HTLV-I infection, HAM rat disease did not occur. In earlier studies, we obtained the morphologic evidence of apoptotic death of oligodendrocytes in affected spinal cords (Seto *et al*, 1995) and the selective

Address correspondence to T. Yoshiki, Department of Pathology/Pathophysiology, Division of Pathophysiological Science, Hokkaido University Graduate School of Medicine, Kita-15, Nishi-7, Kita-ku, Sapporo 060-8638, Japan. E-mail: path1@med.hokudai.ac.jp

X. Jiang is currently in the Department of Surgery, University of Washington, Box 357740, Seattle, WA 98195, USA. O. Ohya is currently in the Zeria Pharmaceutical Co., Ltd., Nihonbashi, Tokyo 103-8351, Japan.

The authors thank Tsutomu Osanai and the entire staff of Institute for Animal Experimentation, Hokkaido University Graduate School of Medicine, for maintenance of HTLV-I carrier rats; Kenichi Nakase for technical assistance; and Mariko Ohara for language assistance. This work was supported by Ministries of Education, Culture, Sports, Science and Technology, and Health, Labour and Welfare of Japan.

Received 9 September 2002; revised 5 March 2003; accepted 22 April 2003.

expression of the HTLV-I *pX* mRNA in the affected spinal cords and peripheral nerves (Tomaru *et al*, 1996). In chronological histopathological studies, we identified apoptotic cells in spinal cords of HTLV-I–infected WKAH carriers, even from early asymptomatic stages of the disease, about 7 months after the induced infection (Ohya *et al*, 2000). Among several cytokines, mRNA expression and protein production of tumor necrosis factor (TNF)-α were evident in the affected spinal cords and cerebrospinal fluid. The majority of HTLV-I–infected cells in the spinal cord were the microglia/macrophage lineage cells, one of the TNF-α–producing cells in the central nervous system (CNS) (Kasai *et al*, 1999; Jiang *et al*, 2000). Collective evidence indicated that the selective activation of HTLV-I, in particular Tax expression, and production of TNF-α, probably by HTLV-I–infected microglia/macrophage lineage cells, are causally related to apoptotic death of oligodentrocytes, a major pathogenetic pathway of the HTLV-I–induced myeloneuropathy.

In the present work, we examined molecular expression of candidate genes involved in apoptosis of oligodendrocytes, using a semiquantitative reverse transcriptase–polymerase chain reaction (RT-PCR) method. We also examined these genes in spinal cords of resistant strains with HTLV-I infection, for a comparative analysis.

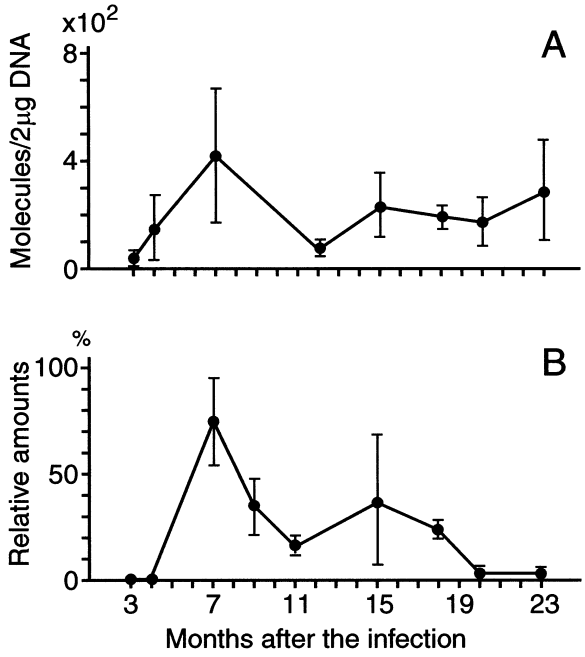

Figure 1 Chronological semiquantitative analyses of HTLV-I provirus DNA (**A**) and *pX* mRNA (**B**) in the spinal cord of WKAH rats with HTLV-I infection. (**A**) Competitive PCR by PX1 primer pair was carried out on 2 μg of DNA from each spinal cord of HTLV-I–infected WKAH rats. (**B**) RT–competitive PCR by RPX primer pair and Southern blot method was carried out on 100 ng of total RNA from each spinal cord of HTLV-I–infected WKAH rats. Relative amounts of the HTLV-I *pX* mRNA were measured against the maximum expression level as 100. **A** and **B**, the mean amounts of least three rats at each month after the infection were calculated and plotted on the graphs. Bars mean standard deviation.

Results

Chronological analyses of amounts of HTLV-I provirus DNA and pX *mRNA in spinal cords of HTLV-I–infected WKAH rats*

To determine the possible participation of HTLV-I infection in the pathogenetic process of HAM rat disease, amounts of the provirus DNA and expression levels of the *pX* mRNA were measured in spinal cords of HTLV-I–infected WKAH rats at each month after the infection, using competitive PCR and RT–competitive PCR (Figure 1). In peripheral blood mononuclear cells (PBMCs), the provirus DNA was detected at least from 1 month after the infection, but was not evident in the spinal cords before 3 months after the infection by our competitive PCR method (data not shown). Although provirus DNA was consistently detected in the spinal cords from 4 to 23 months after the infection, the amounts of provirus DNA increased at a peak (about 400 molecules in 2 μg of the spinal cord DNA) in the early asymptomatic stage of disease course, about 7 months after infection (Figure 1**A**). Relative amounts of *pX* messages also changed, in a similar pattern with that of provirus DNA from 3 to 18 months, thereafter only minimal levels of *pX* messages were evident, although provirus DNA was consistently observed at about 200 molecules in 2 μg of the DNA (Figure 1**B**). In this early asymptomatic period, no significant histological findings were observed in spinal cords except for a few apoptotic oligodendrocytes.

Chronological analysis of expression of apoptosis-associated genes in spinal cords of HTLV-I–infected WKAH rats

Because apoptotic death of oligodendrocytes in spinal cords of HAM rat disease strongly correlated to the development of demyelination (Seto *et al*, 1995; Ohya *et al*, 2000), we examined apoptosis-related host genes, including TNF-α, *bcl-2*, *bax*, and *p53*, using RT–competitive PCR. The expression of TNF-α mRNA increased gradually starting at 7 months after the infection (Figure 2). Although the expression of TNF-α mRNA was occasionally detected in the spinal cord of uninfected control rats by RT-PCR, it was out of detection levels by our competitive RT-PCR (data not shown). Levels of *bcl-2* mRNA expression in spinal cords of HTLV-I–infected WKAH rats were strongly suppressed from 7 to 12 months and the expression gradually recovered after 15 months (Figure 3). In untreated control rats, the expression was consistently high throughout their lifetime and was gradually increased in senescent rats after 15 months of age. Levels of the *bax* mRNA expression

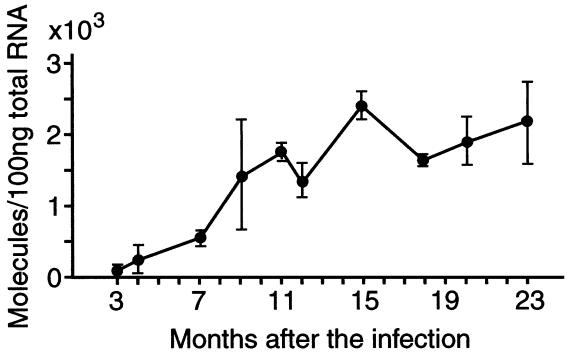

Figure 2 Chronological analysis of expression level of TNF-α mRNA in the spinal cord of WKAH rats with HTLV-I infection. Semiquantitative amounts of TNF-α mRNA in 100 ng of total RNA from spinal cords of WKAH rats at each month after the infection were measured, using RT–competitive PCR.

in HTLV-I–infected WKAH rats changed, with a pattern similar to the findings in case of *bcl-2* mRNA (Figure 4**A**). On the other hand, levels of the *p53* mRNA expression in HTLV-I–infected WKAH rats were more than twice as high, compared to findings in control rats at all ages examined (Figure 4**B**).

Comparison of amounts of provirus DNA and pX*, TNF-α, and* bcl-2 *mRNAs in spinal cords between the HAM-susceptible WKAH strain and other HAM-resistant strains*

Although all rat strains tested were susceptible to HTLV-I infection, HAM rat disease developed only in WKAH strain rats (Ishiguro *et al*, 1992). To investigate the role of HTLV-I infection and apoptosis-related genes in the pathogenesis, we compared the chronological distribution of amounts of provirus DNA and *pX*, TNF-α, and *bcl-2* mRNAs in spinal cords between the HAM-susceptible WKAH strain and the HAM-resistant ACI and LEW strains with HTLV-I infection. Using PCR, HTLV-I provirus DNA was frequently detected in spinal cord of all rat strains examined, WKAH (26/26), ACI (12/14), and LEW (10/14) (Table 1). However, the amounts of provirus DNA in the spinal cords of ACI and LEW rats were smaller than that in WKAH rats throughout their lifetime and the provirus expansion observed in WKAH rats did not occur in ACI and LEW rats (Figures 1**A** and 5**A**). On the other hand, in the cerebrum, which is unaffected by HTLV-I infection (Ishiguro *et al*, 1992), no significant difference in amounts of provirus was observed among these three strains and amounts were less than 100 molecules in 2 μg DNA (Figure 6; Student's *t* test). In other unaffected tissues such as kidney and spleen (Ishiguro *et al*, 1992), the amounts were also less than 100 molecules in 2 μg DNA, with similar levels among strains (data not shown). As a result of examination of HTLV-I *pX* mRNA by RT-PCR, *pX* mRNA was found to be selectively expressed in spinal cords of WKAH rats (20/26), but was detected

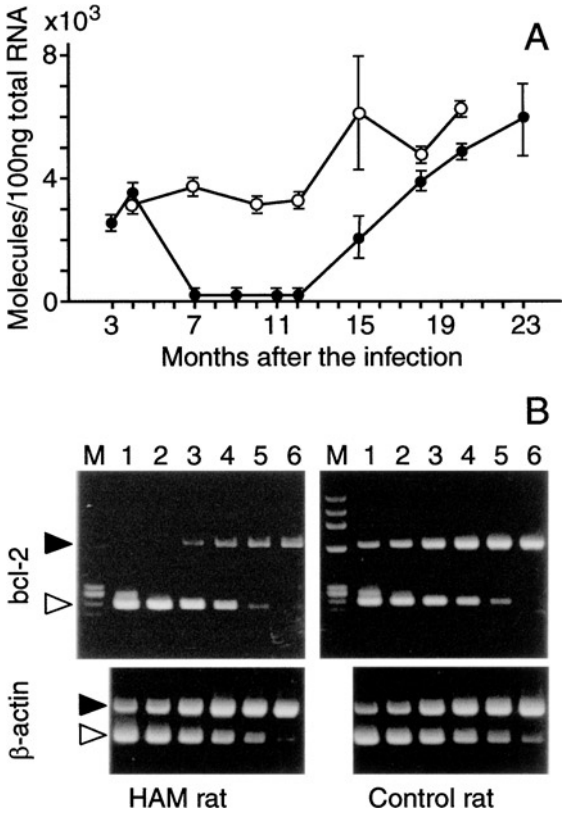

Figure 3 Chronological analysis of expression level of *bcl-2* mRNA in the spinal cord of WKAH rats with HTLV-I infection. (**A**) Semiquantitative amounts of *bcl-2* mRNA in 100 ng of total RNA from spinal cords of HTLV-I–infected WKAH carrier rats (●) at each month after the infection were measured using RT–competitive PCR and findings compared with those of untreated WKAH control rats (○). Horizontal axis of control rats shows the age in months. (**B**) A representative result of RT–competitive PCR for *bcl-2* mRNA is shown (*upper figures*). Each 100 ng of total RNAs from spinal cords of a WKAH carrier rat at 12 months after the infection and of an age-matched untreated control rat were amplified under conditions of the RT–competitive PCR method. Lanes 1 to 6 for *bcl-2* contain 10, 1, 10^{-1}, 10^{-2}, 10^{-3}, and 10^{-4} attomole of bcl-2 MIMIC, respectively. Lower figures show results of RT–competitive PCR for β-actin as a control. Lanes 1 to 6 for β-actin contain 100, 10, 1, 10^{-1}, 10^{-2}, and 10^{-3} attomole of β-actin MIMIC. *Closed arrows* indicate the amplified products of *bcl-2* (639 base pairs [bp]) or β-actin (591 bp) and *open arrows* indicate each competitor against *bcl-2* (230 bp) or β-actin (347 bp). M is a φ*X174* with *Hae*III digestion size marker.

in only 1 of 14 rats in each HAM-resistant strain (Table 1). The expression levels in the two HAM-resistant rats were under the minimal limit of sensitivity of the competitive RT-PCR we used (under 9 molecules per 100 ng of total RNA; data not shown). Levels of TNF-α mRNA expression in spinal cords of HTLV-I–infected WKAH rats gradually increased from 7 to 23 months after the infection (see Figure 2), but those of HTLV-I–infected ACI and LEW rats were consistently low (Figure 5**B**). Expression of the *bcl-2* mRNA in spinal cords of both HTLV-I–infected HAM-resistant strains tended to be at higher compared with findings in untreated controls. The suppression of

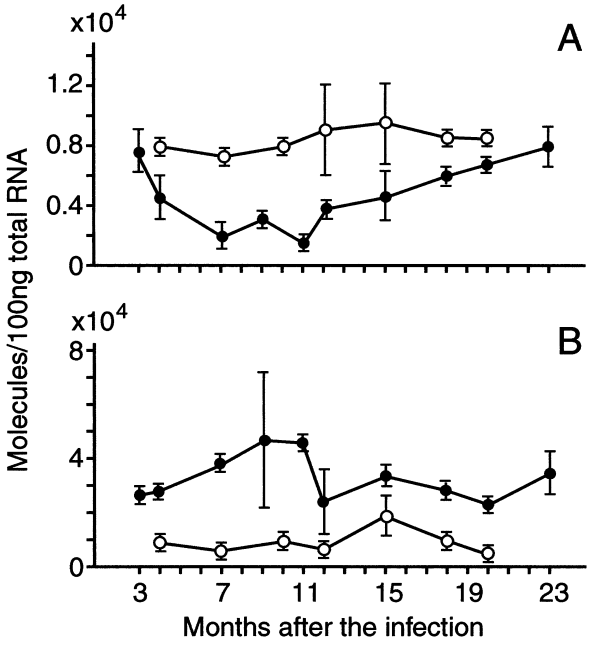

Figure 4 Chronological analyses of semiquantitative amounts of *bax* and *p53* mRNAs in spinal cords of WKAH rats with HTLV-I infection. Semiquantitative amounts of *bax* (**A**) and *p53* (**B**) mRNAs in 100 ng of total RNA from spinal cords were measured using RT–competitive PCR with gene specific primer pairs and two-fold dilution series of each bax or p53 MIMIC. Both HTLV-I carrier (●) and untreated WKAH rats (○) were examined.

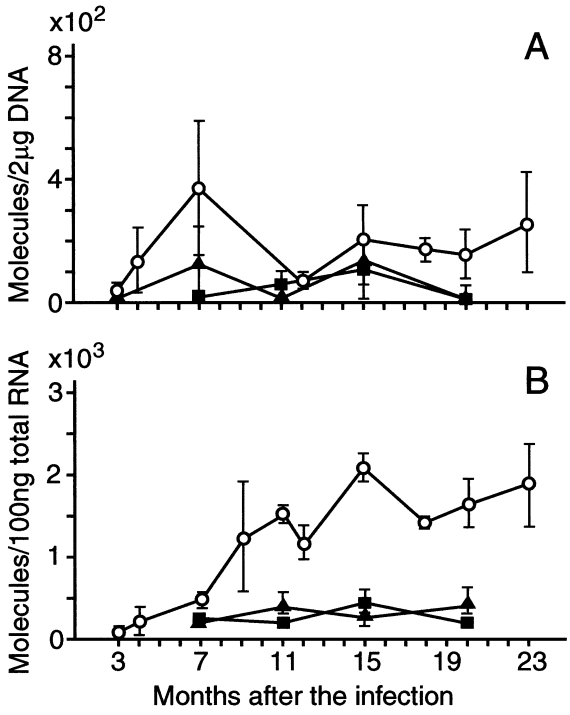

Figure 5 Chronological analyses of the provirus load (**A**) and levels of TNF-α mRNA (**B**) in spinal cords of HAM-resistant strains, ACI (▲) and LEW (■) rats, with HTLV-I infection. To compare with HAM-susceptible strain, results of HTLV-I–infected WKAH rats (○) were placed in the figures.

that seen in WKAH rats with HTLV-I infection was not evident in either strain (Figure 7).

Histopathology of spinal cords of HTLV-I–infected WKAH, ACI, and LEW strain rats

The initial change in spinal cord lesions in HTLV-I–infected WKAH rats was the presence of apoptotic cells, first observed at about 7 months after the infection and thereafter, whereas focal demyelination, vacuolar change, and macrophage infiltration were present in anterior and lateral funiculi from age 15 months then gradually progressed. These pathological features were similar to our previous study (Ohya *et al*, 2000). However, no histopathological lesion was evident in spinal cords of HTLV-I–infected ACI and LEW rats, as compared with that of each control throughout their lifetime (data not shown).

Table 1 Detection of provirus DNA and *pX* mRNA in spinal cords of WKAH, ACI, and LEW rats with HTLV-I infection

Strains	*HAM rat disease*	*Number of rats*	*Provirus DNA*[a]	pX *mRNA expression*[b]
WKAH	Susceptible	26	26/26[c]	20/26
ACI	Resistant	14	12/14	1/12
LEW	Resistant	14	10/14	1/12

[a]Detection of provirus DNA was done using Southern hybridization after PCR amplification.
[b]pX mRNA was detected using Southern hybridization after RT-PCR amplification.
[c]Number of positive/number of rats used.

Discussion

Our preceding studies indicated that the major pathogenetic pathway of HAM rat disease appeared to be

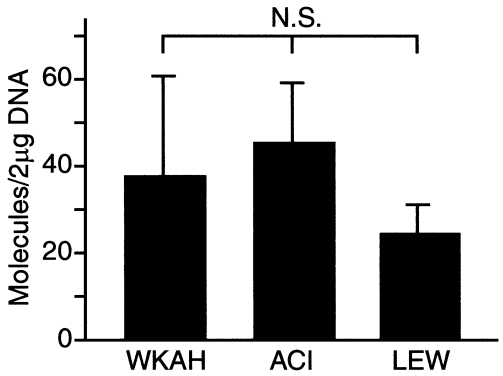

Figure 6 Comparison of semiquantitative amounts of HTLV-I provirus molecule in cerebrum between HAM-susceptible WKAH and resistant ACI and LEW rats with HTLV-I infection. Two micrograms of each DNA from cerebrum of WKAH ($n = 4$), ACI ($n = 3$), and LEW ($n = 3$), rats at 7 to 9 months after HTLV-I infection and a series of serially diluted PX1 MIMIC were amplified by competitive PCR with a PX1 primer pair. No statistical significance was evident (NS, Student's *t* test).

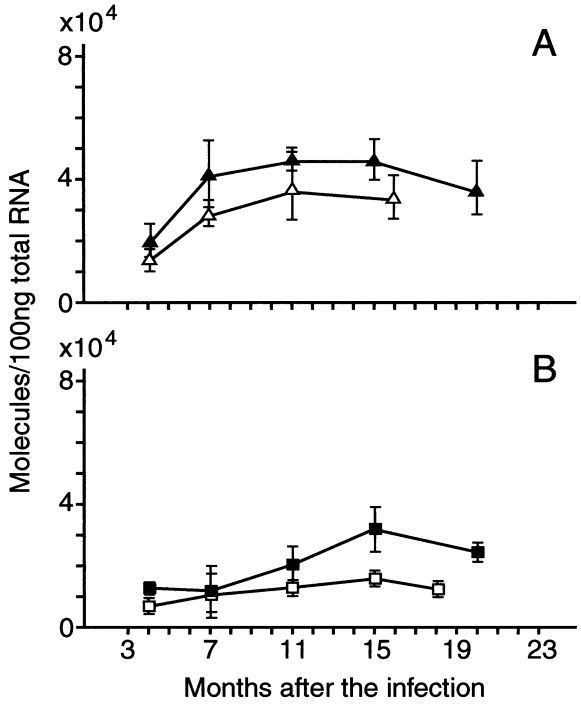

Figure 7 Chronological analyses of semiquantitative amounts of *bcl-2* mRNA in the spinal cords of ACI (**A**) and LEW (**B**) rats with HTLV-I infection. ▲ and ■ show HTLV-I–infected ACI and LEW rats, respectively. Untreated ACI (△) and LEW (□) rats served as controls.

closely related to apoptotic cell death of oligodendrocytes and to the selective activation of HTLV-I *pX* and production of TNF-α in target spinal cords and peripheral nerves (Seto *et al*, 1995; Tomaru *et al*, 1996; Ohya *et al*, 2000). The high HTLV-I provirus load appears to be a major pathogenetic factor in the development of human HAM/TSP in HTLV-I carriers, because amounts of the HTLV-I provirus DNA in PBMCs of HAM/TSP patients were high as compared to findings in asymptomatic HTLV-I carriers (Nagai *et al*, 1998). In the present study, the provirus DNA was first detected in the spinal cords at 3 months after infection, though it has been consistently evident in the PBMCs from 1 month after the infection. In line with this observation, Kanzanji *et al* (2000) reported that in sequirrel monkeys given intravenous infection of HTLV-I, the provirus DNA was consistently detected in the PBMCs from 3 weeks after infection, but was almost nil before 35 days after infection in all other tissues except for lymphoid tissues, including thoracic spinal cords. In the present study, amounts of provirus DNA in the spinal cord of HAM-susceptible WKAH strain increased in connection with increment of *pX* expression, which peaked in the early asymptomatic stage (around 7 months after the infection), and were consistently higher than those of HAM-resistant ACI and LEW strains. Because no significant difference was evident in amounts in other unaffected tissues, such as cerebrum, among the three strains, the provirus expansion was specific in the spinal cord of HAM-sensitive WKAH rats. This selective increment of provirus load with *pX* expression appears to be the most important factor in the development of HAM rat disease, although it is not yet clear why HTLV-I provirus increases selectively in the spinal cords of WKAH rats. Earlier studies demonstrated that the major HTLV-I–infected cells in the spinal cords were microglia/macrophage lineage cells (Kasai *et al*, 1999; Jiang *et al*, 2000), although the major reservoir of HTLV-I in our model is lymphoid tissues. Microglia/macrophages are major cells capable of TNF-α production in the CNS (Lee *et al*, 1993), and the p40Tax-encoded HTLV-I *pX* region transactivates many cellular genes, including TNF-α (Albrecht *et al*, 1992). Actually, TNF-α expression in spinal cords of HTLV-I–infected WKAH rats began to increase from about 7 months after the infection. TNF-α induces apoptosis through activation of the death domain of TNF receptor 1 (TNFR1; reviewed by Smith *et al*, 1994). Eugster *et al* (1999) demonstrated that stimulation of TNFR1 by TNF-α is a more crucial factor for demyelination of spinal cord than the number of inflammatory perivascular cuffs in myelin oligodendrocyte glycoprotein-induced experimental autoimmune encephalitis, using knockout mice lacking TNF-α, TNFR1, TNFR2 or TNFR1 and 2. TNF-α directly causes cellular damage (probably apoptosis) to oligodendrocytes *in vitro* (Selmaj *et al*, 1991; Wilt *et al*, 1995), and the sensitivity to TNF-α–induced apoptosis of oligodendrocytes is increased in spinal cords with HTLV-I infection (Jiang *et al*, 2000). Collective evidence suggests that TNF-α production transactivated by *pX* expression, with provirus expansion in the infected microglia/macrophage lineage cells, may induce the pathogenetic apoptosis of oligodendrocytes in spinal cords of HTLV-I–infected WKAH rats. In the late stage, TNF-α expression continued at high levels, although *pX* message decreased gradually. It is more likely that TNF-α production at the late stage is produced by infiltrating and accumulating activated microglial/macrophage lineage cells, which may include many noninfected cells as scavengers, observed in the affected lesion (Ohya *et al*, 2000). In HAM/TSP patients, the main infected cells were demonstrated to be infiltrating lymphocytes or astrocytes (Hara *et al*, 1994; Lehky *et al*, 1995), although HTLV-I can infect all types of glial cells *in vitro* (Watabe *et al*, 1989; Hoffman *et al*, 1992). It is also to be noted that in the affected spinal cord of HAM rats, lymphocytic infiltration was not observed throughout the disease process (Ishiguro *et al*, 1992; Seto *et al*, 1995). Therefore, in the affected spinal lesion of our rat model, it appears that the infected microglia/macrophages predominate.

Many cellular genes are involved in the regulation of apoptotic cell death. Major apoptosis-related genes, *bcl-2*, *bax*, and *p53*, were investigated in the spinal cord of HTLV-I–infected WKAH rats. The mRNA level of apoptosis-resistant *bcl-2* gene was

markedly decreased from 7 to 12 months after the infection, in close association with the expansion of provirus load and the increment of *pX* expression. Expression of TNF-α and appearance of apoptotic oligodendrocytes also began around this time. Our recent study also showed evidence of *bcl-2* down-regulation in *in vitro*–separated oligodendrocytes (Jiang *et al*, 2000). In line with this observation, in Tax-transformed Rat-1 cells, HTLV-I Tax-mediated apoptotic cell death, under serum-deprived conditions, was effectively blocked by expression of *bcl-2* (Yamada *et al*, 1994). On the other hand, expression of TNF-α seems to inversely correlate with down-regulation of *bcl-2*. Namely, by transduction of TNF-α gene into human lymphoma T-cell line, apoptotic cell death is induced by down-regulation of the *bcl-2* gene (Gillio *et al*, 1996). In human brain aggregate cultures, following TNF-α treatment, Bcl-2 protein is significantly decreased (Pulliam *et al*, 1998). Collective evidence suggests that the expression of TNF-α and the severe suppression of apoptosis-resistant *bcl-2* expression in the spinal cord of HTLV-I–infected WKAH rats, especially in oligodendrocytes, may be closely associated with apoptotic death of oligodendrocytes. In the late stage of human HAM/TSP, *bcl-2* expression was shown to increase in many infiltrating T lymphocytes, and the high expression of *bcl-2* seems to protect apoptosis of infiltrating T lymphocytes and prolong the inflammatory process (Umehara *et al*, 1994). However, there is no report demonstrating such findings in the initial stage before developing of disease in humans. Although HAM rat disease may not recapitulate exactly the human condition with HAM/TSP, *bcl-2* down-regulation and apoptosis of oligodendrocytes shown in our rat model may initiate to induce infiltration of T lymphocytes with high *bcl-2* expression, resulted in the progression of the spinal damage and development of the symptom in human HAM/TSP. The increment of *bcl-2* expression in noninfected senescent control rats might indicate accumulating of microglia/macrophage linage cells with aging in this particular strain (Ohya *et al*, 2000).

On the other hand, an apoptosis promoting gene, *bax*, was also repressed in the spinal cords of HTLV-I–infected WKAH rats. It may be consistent with the observation by Brauweiler *et al* (1997) that Tax mediates repression of *bax*, although no repression of *bax* expression was reported in HTLV-I–transformed T cells or lymphocytes from ATL patients (Nicot *et al*, 2000). The *p53* tumor suppressor gene, which is critical for controls of cell proliferation and apoptosis, consistently expressed at high levels in the spinal cord of HTLV-I–infected WKAH rats. The elevation of *p53* protein expression was noted in tumors derived from HTLV-I tax transgenic mice (Hall *et al*, 1998) or in Tax-immortalized T cells (Akagi *et al*, 1997). However, it was demonstrated that function of the elevated *p53* expression is inactivated with stabilization of wild-type *p53* by Tax, despite the absence of genetic mutation (Reid *et al*, 1993; Pise-Masison *et al*, 1998). Therefore, the function of up-regulated *p53* in HAM rats may also be inactivated by Tax, although it is not yet identified which type of cells expresses up-regulation of *p53*.

The pathogenesis underlying chronic progressive myeloneuropathy in our rat model may provide new insights into the pathogenesis of neural demyelinating diseases, including human HAM/TSP, associated with deregulation of cell growth–related genes, especially those involved in the control of apoptosis regulatory networks. Recently, Levin *et al* (2002) indicated that anti-Tax antibody in HAM/TSP might play as a cross-reactive autoantibody against the neuron-specific hnRNP-A1 molecule and might cause the functional damage of neurons. Our rat model is also useful to clarify whether such molecular mimicry plays a role in the pathogenesis of HAM/TSP.

Materials and methods

Animals and HTLV-I infection

Inbred WKAH, ACI, and LEW strain rats were obtained from the Institute for Animal Experimentation, Hokkaido University Graduate School of Medicine. All animal experiments were done based on the *Guide for Care and Use of Laboratory Animals* set up by Hokkaido University Graduate School of Medicine. HTLV-I–infected rats in all strains used were produced by injection of MT-2 cells (an immortalized human T-cell line producing HTLV-I) (Miyoshi *et al*, 1981) to newborn rats (Ishiguro *et al*, 1992). At 1 month after the injection, the presence of HTLV-I infection in PBMCs was confirmed by PCR–Southern blots, using HTLV-I–specific oligonucleotide primers and probe (Ishiguro *et al*, 1992). No human specific sequence was detected in PBMCs of the infected rats by PCR. Each carrier rat was killed at 3, 4, 7, 9, 11, 12, 15, 18, 20, and 23 months after the induced infection. Untreated rats of each strain, at comparable ages, served as normal controls. At least 3 rats were used in each experiment. All HTLV-I–infected rats were maintained under the P3 level.

Prior to preparation of tissue samples, all rats were perfused with 500 ml of ice-cold phosphate-buffered saline with heparin following anesthetization with sodium pentobarbital. Each organ was subdivided for DNA and RNA extraction and for histological examinations.

Detection of HTLV-I provirus DNA and pX *mRNA in the spinal cord*

PCR–Southern blots were made to examine the integration of HTLV-I provirus DNA in nervous tissues, as described (Ishiguro *et al*, 1992). Total RNA was purified using ISOGEN (Nippon Gene, Tokyo, Japan) and the RT-PCR–Southern blots to detect the expression

of *pX* mRNA, according to reported methods (Tomaru *et al*, 1996).

Semiquantitative analysis of provirus DNA in the spinal cord

Amounts of provirus DNA in the spinal cord were measured using competitive PCR (Siebert and Larrick, 1992). The competitor was generated using PCR MIMIC Construction Kits (Clontech Lab., Palo Alto, CA, USA). An internal DNA standard (MIMIC) was synthesized by PCR amplification of a neutral intervening DNA (*v-ervB*) with composite sense and antisense primers constructed at each 5′ end of *v-ervB*–specific sense and antisense primer sequences binding with the HTLV-I *pX* gene–specific sense and antisense primers (PX1), respectively (Table 2). For sensitive discrimination, the PX1 primer pair was biotinylated. Two micrograms of extracted DNA and serially twofold diluted PX1 MIMIC DNA (from 2×10^{-2} attomole) were amplified together, with fluorescence thiocyanate-conjugated sense and antisense PX1 primers at 40 cycles, using a *Taq* polymerase (Takara Shuzo, Kyoto, Japan) and according to the manufacturer's instructions at 94°C for 1 min, 63°C for 1 min, and 72°C for 1 min. The PCR products were electrophoretically separated on 5% polyacrylamide gels and each amplified fragment of the *pX* gene and MIMIC DNA was detected using a fluoroimaging analyzer (FluoroImager, Molecular Dynamics Japan, Tokyo, Japan). The amount of molecules of provirus DNA in each sample was estimated from the amount of MIMIC competitor, as described elsewhere (Katsumata *et al*, 1999).

Semiquantitative analysis of the pX*, TNF-α,* bcl-2*,* bax*, and* p53 *mRNAs in the spinal cord*

For semiquantification of mRNA expression, competitive PCR after RT (competitive RT–PCR) was done. Gene-specific oligonucleotide primers for *pX* (RPX), TNF-*α*, *bcl-2*, *bax*, and *p53*, and each composite primer pair for synthesizing MIMIC (RPX MIMIC, TNF-*α* MIMIC, bcl-2 MIMIC, bax MIMIC, and p53 MIMIC), are given in Table 2. cDNA reversely transcribed from 100 ng of each total RNA of spinal cords and serially diluted each MIMIC (2-fold or 10-fold in each target) were coamplified, with each gene-specific sense and antisense primer pair at 35 cycles using *Taq* polymerase (Takara) and according to the manufacturer's instructions at 94°C for 1 min, 63°C for 1 min, 72°C for 1 min. The PCR products were electrophoresed on a 2% agarose gel containing ethidium bromide and were visualized under an ultraviolet lamp. The density of amplified bands was measured using a flat bed scanner (HP Scan Jet 3c/t, Hewlett Packard, Palo Alto, CA) and NIH image. The amount of molecules of each target cDNA (approximately equivalent to that of target mRNA),

Table 2 Gene-specific primers and composite primers used

Target	*Gene-specific primers (5′ to 3′)*	*Composite primers for MIMIC DNA (5′ to 3′)*
HTLV-I provirus (PX1)	Sense gtcttcttttcggatacccagtcta	gtcttcttttcggatacccagtctacgcaagtgaaatctcctccg
	Antisense (205)[a] aaggaggggagtcgagggatataagga	(450) aaggaggggagtcgagggataaggatctgtcaatgcagtttgtag
pX (RPX)	Sense atccccgtggagactcctcaa	atccccgtggagactcctcaacaagtttcgtgagctgattg
	Antisense (144) aacacgtagactgggtatcc	(320) aacacgtagactgggtatcctctgtcaatgcagtttgtag
TNF-*α*	Sense ggaaagcatgatccgagatg	ggaaagcatgatccgagatgtgttatacagggagatgaaa
	Antisense (682) aaagtagacctgcccggact	(260) aaagtagacctgcccggacttctgtcaatgcagtttgtag
bcl-2	Sense gccgggagaacagggtatgataacc	gccgggagaacagggtatgataacccaagtttcgtgagctgattg
	Antisense (639) cgtcttcagagacagccaggagaaa	(230) cgtcttcagagacagccaggagaaagggacaagatactcatctgc
bax	Sense caccaagaagctgagcgagtgtc	caccaagaagctgagcgagtgtccagtttcgtgagctgattg
	Antisense (273) tcccggaggaagtccagtgtcca	(126) tcccggaggaagtccagtgtccatttcatctccctgtataaca
p53	Sense aggttcgtgtttgtgcctgtcctg	aggttcgtgtttgtgcctgtcctgcgcaagtgaaatctcctccg
	Antisense (291) agctggagtgagccctgctgtctc	(448) agctggagtgagccctgctgtctctctgtcaatgcagtttgtag
β-Actin	Sense atgggtcagaaggcctcctacgt	atgggtcagaaggcctcctacgtcgcaagtgaaatctcctccg
	Antisense (591) aggcagctcatagctcttctccag	(347) aggcagctcatagctcttctccaggggacaagatactcatctgc

[a]Molecular size (base pairs) of each PCR product is shown in parentheses.

except for *pX*, was calculated using the same method described above. For measurement of the *pX* expression, standard Southern hybridization was done using radioactively labeled oligonucleotide probes, TTTCTTTGGGATCGGCGGGG for the amplified *pX* cDNA and AACAAGATAGCGGGGAGGGT for the RPX MIMIC DNA (the Tm value was close to the probe for *pX*), after electrophoresis. After autoradiography, the density of each specific amplified band was measured using a flat bed scanner (HP Scan Jet 3c/t) and NIH image. Relative amounts of *pX* mRNA are given as percent ratios against the maximum amount as one. In each sample, amounts of the β-actin mRNA were quantified by the competitive RT-PCR, as a control for RNA preparation. The β-actin oligonucleotide primers and the composite primers are also given in Table 2.

Histopathology

Hematoxylin and eosin and Kluver-Barrera stains were used. For *in situ* detection of apoptotic cells, the terminal deoxynucleotidyl transferase–mediated dUTP-biotin nick end labeling was done, as described (Seto *et al*, 1995).

References

Akagi T, Ono H, Tsuchida N, Shimotohno K (1997). Aberrant expression and function of p53 in T-cells immortalized by HTLV-I Tax1. *FEBS Lett* **406:** 263–266.

Albrecht H, Shakhov AN, Jongeneel CV (1992). *trans*-Activation of the tumor necrosis factor alpha promoter by the human T-cell leukemia virus type I Tax1 protein. *J Virol* **66:** 6191–6193.

Brauweiler A, Garrus JE, Reed JC, Nyborg JK (1997). Repression of *bax* gene expression by the HTLV-I Tax protein: implications for suppression of apoptosis in virally infected cells. *Virology* **231:** 135–140.

Eugster H-P, Frei K, Bachmann R, Bluethmann H, Lassmann H, Fontana A (1999). Severity of symptoms and demyelination in MOG-induced EAE depends on TNFR1. *Eur J Immunol* **29:** 626–632.

Gessain A, Barin F, Vernant JC, Gout O, Maurs L, Calender A, de The G (1985). Antibodies to the human T cell lymphotropic virus type I in patients with tropical spastic paraparesis. *Lancet* **8452:** 407–410.

Gillio TA, Cignetti A, Rovera G, Foa R (1996). Retroviral vector-mediated transfer of the tumor necrosis factor alpha gene into human cancer cells restores an apoptotic cell death program and induces a bystander-killing effect. *Blood* **87:** 2486–2495.

Hall AP, Irvine J, Blyth K, Cameron ER, Onions DE, Campbell ME (1998). Tumours derived from HTLV-I tax transgenic mice are characterized by enhanced levels of apoptosis and oncogene expression. *J Pathol* **186:** 209–214.

Hara H, Morita M, Iwaki T, Hatae T, Itoyama Y, Kitamoto T, Akizuki S, Goto I, Watanabe T (1994). Detection of human T lymphotrophic virus type I (HTLV-I) proviral DNA and analysis of T cell receptor Vβ CDR3 sequences in spinal cord lesions of HTLV-I-associated myelopathy/tropical spastic paraparesis. *J Exp Med* **180:** 831–839.

Hoffman PM, Dhib-Jalbut S, Mikovits JA, Robbins DS, Wolf AL, Bergey GK, Lohrey NC, Weislow OS, Ruscetti FW (1992). Human T-cell leukemia virus type-I infection of monocytes and microglial cells in primary human cultures. *Proc Natl Acad Sci U S A* **89:** 11784–11788.

Hollsberg P, Hafler DA (1993). Seminars in medicine of Beth Israel Hospital, Boston. Pathogenesis of diseases induced by human lymphotropic virus type I infection. *N Engl J Med* **328:** 1173–1182.

Ishiguro N, Abe M, Seto K, Sakurai H, Ikeda H, Wakisaka A, Togashi T, Tateno M, Yoshiki T (1992). A rat model of human T lymphocyte virus type I (HTLV-I) infection. 1. Humoral antibody response, provirus integration, and HTLV-I-associated myelopathy/tropical spastic paraparesis-like myelopathy in seronegative HTLV-I carrier rats. *J Exp Med* **176:** 981–989.

Jiang X, Ikeda H, Tomaru U, Morita K, Tanaka Y, Yoshiki T (2000). A rat model for human T lymphocyte virus type I-associated myeloneuropathy: down-regulation of bcl-2 expression and increase in sensitivity to TNF-α of the spinal oligodendrocytes. *J Neuroimmunol* **106:** 105–113.

Kasai T, Ikeda H, Tomaru U, Yamashita I, Ohya O, Morita K, Wakisaka A, Matsuoka E, Moritoyo T, Hashimoto K, Higuchi I, Izumo S, Osame M, Yoshiki T (1999). A rat model of human T lymphocyte virus type I (HTLV-I) infection: in situ detection of HTLV-I provirus DNA in microglia/macrophages in affected spinal cords of rats with HTLV-I-induced chronic progressive myeloneuropathy. *Acta Neuropathol* **97:** 107–112.

Katsumata K, Ikeda H, Sato M, Ishizu A, Kawarada Y, Kato H, Wakisaka A, Koike T, Yoshiki T (1999). Cytokine regulation of env gene expression of human endogenous retrovirus-R in human vascular endothelial cells. *Clin Immunol* **93:** 75–80.

Kazanji M, Ureta-Vidal A, Ozden S, Tangy F, de Thoisy B, Fiete L, Talarmin A, Gessain A, de The G (2000). Lymphoid organs as a major reservoir for human T-cell leukemia virus type 1 in experimentally infected squirrel monkeys (*Saimiri sciureus*): Provirus expression, persistence, and humoral and cellular immune responses. *J Virol* **74:** 4860–4867.

LaGrenade L, Hanchard B, Fletcher V, Cranston B, Blattner W (1990). Infective dermatitis of Jamaican children: a marker for HTLV-I infection. *Lancet* **8727:** 1345–1347.

Lee SC, Liu W, Dickson DW, Brosnan CF, Berman JW (1993). Cytokine production by human fetal microglia and astrocytes. Differential induction by lipopolysaccharide and IL-1β. *J Immunol* **150:** 2659–2667.

Lehky TJ, Fox CH, Koenig S, Levin MC, Flerlage N, Izumo S, Sato E, Raine CS, Osame M, Jacobson S (1995). Detection of human T-lymphotropic virus type I (HTLV-I) tax RNA in the central nervous system of HTLV-I-associated myelopathy/tropical spastic paraparesis patients by in situ hybridization. *Ann Neurol* **37:** 167–175.

Levin MC, Lee SM, Kalume F, Mocos Y, Dohan Jr FC, Hasty KA, Callaway JC, Zunt J, Desiderio DM, Stuart JM (2002). Autoimmunity due to molecular mimicry as a cause of neurological disease. *Nat Med* **8:** 509–513.

Miyoshi I, Kubonishi I, Yoshimoto S, Akagi T, Ohtsuki Y, Shiraishi Y, Nagata K, Hinuma Y (1981). Type C virus

particles in a cord T-cell line derived by co-cultivating normal human cord leukocytes and human leukaemic T-cells. *Nature* **294:** 770–771.

Mochizuki M, Watanabe T, Yamaguchi K, Takatsuki K, Yoshimura K, Shirao M, Nakashima S, Mori S, Araki S, Miyata N (1992). HTLV-I uveitis: a distinct clinical entity caused by HTLV-I. *Jpn J Cancer Res* **83:** 236–239.

Morgan OS, Rodgers-Johnson P, Mora C, Char G (1989). HTLV-I and polymyositis in Jamaica. *Lancet* **8673:** 1184–1187.

Nagai M, Usuku K, Matsumoto W, Kodama D, Takenouchi N, Moritoyo T, Hashiguchi S, Ichinose M, Bangham CR, Izumo S, Osame M (1998). Analysis of HTLV-I proviral load in 202 HAM/TSP patients and 243 asymptomatic HTLV-I carriers: high proviral losd strongly predisposes to HAM/TSP. *J NeuroVirol* **4:** 586–593.

Nicot C, Mahieux R, Takemoto S, Francini G (2000). Bcl-X_L is up-regulated by HTLV-I and HTLV-II in vitro and in ex vivo ATLL samples. *Blood* **96:** 275–281.

Nishioka K, Maruyama I, Sato K, Kitajima I, Nakajima Y, Osame M (1989). Chronic inflammatory arthropathy associated with HTLV-I. *Lancet* **8635:** 441.

Ohya O, Ikeda H, Tomaru U, Yamashita I, Kasai T, Morita K, Wakisaka A, Yoshiki T (2000). Human T-lymphocyte virus type I (HTLV-I)-induced myeloneuropathy in rats: Oligodendrocytes undergo apoptosis in the presence of HTLV-I. *APMIS* **108:** 459–466

Osame M, Usuku K, Izumo S, Ijichi N, Amitani H, Igata A, Matsumoto M, Tara M (1986). HTLV-I associated myelopathy, a new clinical entity. *Lancet* **8488:** 1031–1032.

Pise-Masison CA, Choi KS, Radonovich M, Dittmer J, Kim SJ, Brady JN (1998). Inhibition of p53 transactivation function by the human T-cell leukemia virus type I Tax protein. *J Virol* **72:** 1165–1170.

Poiesz BJ, Ruscetti FW, Gazdar AF, Bunn PA, Minna JD, Gallo RC (1980). Detection and isolation of type-C retrovirus particles from fresh and cultured lymphocytes of a patient with cutaneous T-cell lymphoma. *Proc Natl Acad Sci U S A* **77:** 7415–7419.

Pulliam L, Zhou M, Stubblebine M, Bitler CM (1998). Differential modulation of cell death proteins in human brain cells by tumor necrosis factor alpha and platelet activation factor. *J Neurosci Res* **54:** 530–538.

Reid RL, Lindholm PF, Mireskandari A, Dittmer J, Brady JN (1993). Stabilization of wild-type p53 in human T-lymphocytes transformed by HTLV-I. *Oncogene* **8:** 3029–3036.

Selmaj K, Raine C, Farooq M, Norton WT, Brosnan CF (1991). Cytokine cytotoxicity against oligodendrocytes. Apoptosis induced by lymphotoxin. *J Immunol* **147:** 1522–1529.

Seto K, Abe M, Ohya O, Itakura O, Ishiguro N, Ikeda H, Wakisaka A, Yoshiki T (1995). A rat model of HTLV-I infection: development of chronic progressive myeloneuropathy in seropositive WKAH rats and related apoptosis. *Acta Neuropathol* **89:** 483–490.

Siebert PD, Larrick JW (1992). Competitive PCR. *Nature* **359:** 557–558.

Smith CA, Farrah T, Goodwin RG (1994). The TNF receptor superfamily of cellular and viral proteins: activation, costimulation, and death. *Cell* **76:** 959–962.

Sugimoto M, Nakashima H, Watanabe S, Uyama E, Tanaka F, Ando M, Araki S, Kawasaki S (1987). T lymphocytes alveolitis in HTLV-I-associated myelopathy. *Lancet* **8569:** 1220.

Tomaru U, Ikeda H, Ohya O, Abe M, Kasai T, Yamasita I, Morita K, Wakisaka A, Yoshiki T (1996). Human T lymphocyte virus type I-induced myeloneuropathy in rats: implication of local activation of the *pX* and tumor necrosis factor-α genes in pathogemesis. *J Infect Dis* **174:** 318–323.

Umehara F, Nakamura A, Izumo S, Kubota R, Ijichi S, Kashio N, Hashimoto K, Usuku K, Sato E, Osame M (1994). Apoptosis of tlymphocytes in the spinal cord lesion in HTLV-I-associated myelopathy: a possible mechanism to control viral infection in the central nervous system. *J Neuropathol Exp Neurol* **53:** 617–624.

Vernant JC, Buisson G, Magdeleine J, De Thore J, Jouannelle A, Neisson-Vernant C, Monplaisir N (1988). T lymphocytes alveolitis, tropical spastic paraparesis and Sjogren's syndrome. *Lancet* **8578:** 177.

Watabe K, Saida T, Kim SU (1989). Human and simian glial cells infected by human T-lymphotoropic virus type I in culture. *J Neuropathol Exp Neurol* **48:** 610–619.

Wilt SG, Milward E, Zhou JM, Nagasato K, Patton H, Rusten R, Griffin DE, O'Connor M, Dubois-Dalcq M (1995). In vitro evidence for a dual role of tumor necrosis factor-alpha in human immunodeficiency virus type I encephalopathy. *Ann Neurol* **37:** 381–394.

Yamada T, Yamaoka S, Goto T, Nakai M, Tsujimoto Y, Hatanaka M (1994). The human T-cell leukemia virus type I Tax protein induces apoptosis which is blocked by the Bcl-2 protein. *J Virol* **68:** 3374–3379.

Yoshida M, Miyoshi I, Hinuma Y (1982). Isolation and characterization of retrovirus from cell lines of human adult T-cell leukemia and its implication in disease. *Proc Natl Acad Sci U S A* **79:** 2031–2035.